Published in final edited form as:
J Orthop Res. 2012 January ; 30(1): 28–36. doi:10.1002/jor.21484.

THE RELATIONSHIPS AMONG SPATIOTEMPORAL COLLAGEN GENE EXPRESSION, HISTOLOGY, AND BIOMECHANICS FOLLOWING FULL-LENGTH INJURY IN THE MURINE PATELLAR TENDON

Nathaniel A Dyment, B.S.[1], **Namdar Kazemi, M.D.**[2], **Lindsey E Aschbacher-Smith, M.S.**[3], **Nicolas J. Barthelery, M.S.**[3], **Keith Kenter, M.D.**[2], **Cynthia Gooch, B.S., L.V.T.**[1], **Jason T Shearn, Ph.D.**[1], **Christopher Wylie, Ph.D.**[3], and **David L Butler, Ph.D.**[1]

[1]Biomedical Engineering Program, School of Energy, Environmental, Biological and Medical Engineering, University of Cincinnati, Cincinnati, OH

[2]Department of Orthopaedic Surgery, College of Medicine, University of Cincinnati, Cincinnati, OH

[3]Division of Developmental Biology, Cincinnati Children's Hospital Research Foundation, Cincinnati, OH

Abstract

Tendon injuries are major orthopaedic problems that worsen as the population ages. Type-I (Col1) and type-II (Col2) collagens play important roles in tendon midsubstance and tendon-to-bone insertion healing, respectively. Using double transgenic mice, this study aims to spatiotemporally monitor Col1 and Col2 gene expression, histology and biomechanics up to 8 weeks following a full-length patellar tendon injury. Gene expression and histology were analyzed weekly for up to 5 weeks while mechanical properties were measured at 1, 2, 5, and 8 weeks. At week 1, the healing region displayed loose granulation tissue with little Col1 expression. Col1 expression peaked at 2 weeks, but the ECM was highly disorganized and hypercellular. By 3 weeks, Col1 expression had reduced and by 5 weeks, the ECM was generally aligned along the tendon axis. Col2 expression was not seen in the healing midsubstance or insertion at any time point. The biomechanics of the healing tissue was inadequate at all time points, achieving ultimate loads and stiffnesses of 48% and 63% of normal values by 8 weeks. Future studies will further characterize the cells within the healing midsubstance and insertion using tenogenic markers and compare these results to those of tendon cells during normal development.

Keywords

tendon; collagen; murine; transgenic; healing

INTRODUCTION

Tendon and ligament injuries present a considerable socioeconomic problem that requires innovative treatment solutions.[1] Those having the highest frequency include the rotator cuff tendons, the quadriceps and patellar tendons, and the Achilles tendon.[2] Such injuries can be

Address for Correspondence: Nathaniel A Dyment, University of Cincinnati, Biomedical Engineering Program, School of Energy, Environmental, Biological and Medical Engineering, 2901 Woodside Drive, ML0048, Cincinnati, OH 45221-0048, Phone: (513) 315 – 5024, Fax: (513) 556 – 4162, dymentna@mail.uc.edu.

especially difficult to repair when there is: 1) a degenerative component to the soft tissue[2] and 2) an involvement of the tendon-to-bone insertion site where mechanical stress accumulates.[3] Given the frequency and challenges with traditional repair, tissue engineers have a real opportunity to improve the healing of both acute and chronic injuries to tendon midsubstance and insertions.

Improving tendon tissue engineering designs dictates that we also better understand the natural healing process following injury. Upregulation of type-I (Col1) and type-II (Col2) collagens is important for functional healing as Col1 is the major collagen type found in the tendon midsubstance and Col2 is expressed in the insertion site during development, growth and healing.[4, 5] Immunohistochemistry and quantitative real-time PCR (qPCR) have typically been used to study these collagen types during tendon healing.[6, 7] However, the temporal expression of these genes during healing is still poorly understood on a spatial or cell-by-cell basis.

Natural tendon healing has been investigated in numerous species including rats,[8] rabbits,[9] and sheep.[10] In some studies, investigators have made simple, well-controlled yet not clinically-relevant window defects while others have created more clinically-relevant tendon-to-bone insertional injuries with degenerative features.[8] Our laboratory has been using principles of functional tissue engineering (FTE) to create repairs of central-third patellar tendon (PT) defects that match normal tangent stiffness up to 50% beyond peak *in vivo* forces recorded in the New Zealand White (NZW) rabbit during inclined hopping activities.[11, 12] While the rabbit central-third PT defect allows us to create controlled injuries and reproducibly analyze tissue-engineered repairs, the lack of genetic tools in the rabbit limits our understanding of the biology of natural healing. For this reason, we bred double transgenic Col1/Col2 mice with green fluorescent protein topaz (GFPtpz) and enhanced cyan fluorescent protein (ECFP) reporters to relate spatial and temporal patterns of gene expression with biomechanics during tendon healing.

Thus, the objectives of this study were to monitor changes in: 1) spatiotemporal Col1 and Col2 gene expression patterns, 2) tissue morphology, and 3) healing biomechanics following a full-length, central PT injury in Col1/Col2 double transgenic mice and to compare these natural healing results to contralateral surgical shams and normal PT in age-matched controls. We hypothesized that: 1) Col1 expression would be greatest in the soft tissue within the defect region at earlier time points (1–2 weeks) during matrix deposition but then decrease over time as the tissue remodels; 2) Col2 expression would be greatest at the insertions at earlier time points (1–2 weeks) but also decrease over time; 3) structural and material properties of the defect tissues would be significantly less than normal PT response up to 8 weeks post-surgery.

METHODS

Experimental Design

Tissue morphology, Col1 and Col2 gene expression, and tendon mechanical properties were investigated at 6 different time points post-surgery in sixty-four (64) 20-wk old (19.5±0.2 weeks; mean±SD) double transgenic mice (Table I). Twenty-week old pOBCol3.6GFPtpz (Col1) and pCol2-ECFP transgenic mice, whose creation and genetics were described previously,[13] were chosen because the tendons at this age are large enough to create repeatable defect injuries. Natural healing of a full-length, central PT defect injury was directly compared with healing of a contralateral sham for both histology at 1, 2, 3, 4, and 5 weeks (n=3 each) and biomechanics at 1, 2, 5, and 8 weeks (n= 12–13 each). Inter-animal comparisons were also made against histology (n = 3) and biomechanics (n = 15) from eighteen (18) normal 20-wk old mice.

Surgical Procedure

All animal protocols were approved by the University of Cincinnati IACUC. Each animal was anaesthetized with 4% isoflourane and both hindlimbs were aseptically prepped. Using loupes (2.5X), anteromedial skin incisions were made over each patellar tendon. Medial and lateral borders of each PT were longitudinally incised (see supplementary video). A jewelers forceps was slipped beneath the tendon and spread to lift the tendon from the knee joint without excessive tension. A longitudinal incision in the tendon was made to create the lateral border of the defect. The jewelers forceps was inserted through the lateral incision and pushed through the tendon to create the medial border of the defect. This incision was extended by sliding the forceps from proximal to distal ends so that the central portion of the tendon could be grasped with tissue forceps and cut at each insertion. A scalpel was used to repeatedly disrupt the insertions at both the patellar and tibial ends until bleeding was induced. In the contralateral limb, a sham procedure was performed by slipping the forceps beneath the tendon without creating the defect. Both limbs were closed with 5-0 prolene suture. Subjects were allowed full range of motion in individual cages following surgery. Each animal was euthanized by CO_2 asphyxiation and the limbs were harvested for histological or biomechanical analysis.

Histological Analysis

Following euthanasia, the femur and tibia were cut mid-shaft and the skin removed. Samples were fixed in 4% paraformaldehyde (Fisher Scientific, Pittsburgh, PA) for 4 hours at 4°C. The limbs were decalcified in 0.5M EDTA/PBS solution (Sigma-Aldrich Corp., St Louis, MO) for 7 days at 4°C, washed 3X in 1X PBS, embedded in OCT media (Andwin Scientific, Addison, IL) and frozen on a metal platform cooled by liquid nitrogen. Sagittal sections (12μm thickness) were made within the healing region of each defect limb. Sham and un-operated control specimens were sectioned in comparable locations. Tissue sections were examined under an inverted fluorescent microscope (Axiovert 25, Carl Zeiss Inc., Göttingen, Germany). Filters for GFPtpz (Exciter - 500/25, Emitter - 545/35, XF104-2; Omega Optical Inc., Brattleboro, VT) and ECFP (Exciter - 440/21, Emitter - 480/30; XF114-2, Omega Optical Inc.) were selected to identify regions of Col1 and Col2 gene expression, respectively. Serial sections were also stained with hematoxylin and eosin (H&E) to visualize tissue morphology.

Five reviewers blindly scored three 10X H&E images from each sample according to a grading system for 1) matrix alignment and 2) cellularity. The reviewers scored each image according to the following scale: 0 indicates normal, 1 indicates mild changes, 2 indicates moderate changes, and 3 indicates marked changes. Individual scores were then averaged together to provide a grade for each criterion.

Biomechanical Analysis

Following euthanasia, animals were frozen at −20°C. On the day of testing, the defect limb was placed at 45° of flexion and the medial/lateral struts were removed. A digital image was taken with a ruler in plane to quantify tendon width. The contralateral PT was then trimmed down to a similar width. The tibia-PT-patella unit was then isolated and the thickness was measured from a digital image taken in the sagittal plane. The tibia was embedded in a custom grip aided with polymethylmethacrylate (Dentsply International, York, PA) and secured with a metal staple over the tibial plateau to prevent slippage or failure at the growth plate. The tibial grip was placed in a materials testing system (100R; TestResources, Shakopee, MN) and the patella was lowered into a custom conical-shaped grip within a PBS bath at 37°C (Fig. 1C–D). Each specimen was preloaded (0.02N), preconditioned (25 cycles, 0–1% strain, 0.003mm/sec), and failed in uniaxial tension (0.003mm/sec) while recording grip-to-grip displacement and load.

Statistical Analysis

Comparisons against normal and comparisons among the defect groups over time were made for structural and materials properties via independent student t-tests with a bonferroni correction for multiple comparisons.[14] A total of nine comparisons were made with a significance level of $p = 0.006$. All statistics were performed using SPSS 13.0 (Chicago, IL).

RESULTS

Surgery and Gross Examination Following Injury

The surgeries succeeded 89.3% of the time, with only eight animals showing lameness or ruptured tendons following the injury. Therefore, a total of 72 animals were required to complete this 64-subject study. Tendon defect width (0.63 ± 0.13mm, mean ± SD) averaged 42% of total PT width (1.50 ± 0.29mm). The natural healing site was slightly translucent at 1 week but was opaque and consistently darker compared to the surrounding native struts at all time points thereafter up to 8 weeks (Fig. 1).

Histological Analysis

The defect tissue at 1 week post-surgery consisted of loose granulation tissue with inflammatory cells, areas of neovascularization, marked reduction in matrix alignment and marked increase in cellularity (Figs. 2B & 3B). After 2 weeks, the ECM was denser but still highly disorganized and hypercellular (Figs. 2C & 3C). Nuclei were hypertrophic and inflammatory cells were still present within the midsubstance of the tendon (Figs. 2B–C & 3B–C). At 3 weeks, the ECM showed improved alignment with only mild to moderate changes but remained mildly hypercellular (Figs. 2D & 3D). The defect at 4–5 weeks post-surgery exhibited a more aligned ECM that appeared similar to normal PT by H&E (Figs. 2E–F & 3E–F).

Semi-quantitative histological scores for matrix and cellular alignment confirmed these qualitative observations. Compared to normal PT (0.33±0.38; mean±SD), early healing tendon matrix was quite disorganized (3.00±0 at 1 week; 2.50±0.58 at 2 weeks; and 1.42±0.63 at 3 weeks) with near normal values by 4 and 5 weeks (0.25±0.32 and 0.33±0.47, respectively). Similarly, compared to normal PT cellularity (0.42±0.50), the healing tissue was hypercellular early (2.75±0.50 at 1 week; 2.42±0.50 at 2 weeks; and 1.25±0.32 at 3 weeks) but more normal at later time intervals (0.92±0.17 at 4 weeks; and 0.17±0.33 at 5-weeks.

Gene expression and cellular morphology varied over time in the defect tendons. Compared to normal PT, Col1 expression at 1 week post-surgery was minimal within the midsubstance but elevated at the insertions (Figs. 2b & 3b,h). Col1 expression peaked at 2 weeks in the midsubstance (Figs. 2c & 3c) with cells appearing more rounded than normal tenocytes. At 3 weeks, expression was still elevated compared to normal but considerably lower than at 2 weeks (Figs. 2d & 3d). Col1 expression did not change much between 3 and 5 weeks post-surgery but cells became more aligned with the tendon axis over time (Figs. 2d–f & 3d–f). Also noteworthy were the bony nodules that formed near the insertions of the healing tissue at multiple time points (Figs. 3H–I & 3h–i). Col1 expression was highly elevated in the hypertrophic cells that lined these nodules (Figs. 3h–i). Blood and marrow also appeared within the nodule at later time points (Fig. 3I). Minimal Col2 expression was observed in these areas (Fig. 3i) and was not present in the tissue midsubstance at any time point.

Compared to normal PT, the contralateral shams were slightly hypercellular but showed a consistently aligned ECM at all time points (Fig. 4A–C). Col1 expression was elevated throughout the length of the tendon at 1 week post-surgery (Fig. 4a). The expression was

reduced by 2 weeks and similar to normal PT expression at 3 weeks and thereafter (Fig. 4b–c).

Biomechanical Analysis

Surgical treatment and time post-surgery each significantly affected the tissue's structural and material properties. Ultimate loads transmitted by the 2-, 5-, and 8-week natural healing tissues were only 37%, 50%, and 48% of normal PT values, respectively ($p < 0.006$; Table II, Fig. 5a). Similarly, stiffnesses for the natural healing tissues were 48%, 62%, and 63% of normal PT ($p < 0.006$). These two structural parameters appeared to reach stable asymptotic values by 8 weeks. In fact, time post-surgery (2, 5, and 8 weeks) had no effect on ultimate load or stiffness of the natural healing tissue. The mode of failure for these specimens was predominantly (94%) soft tissue failures near the distal insertion with the remainder occurring in the tendon midsubstance. Also, the failure mode did not differ among groups and had no effect on mechanical properties. It is important to note that the 1-week defect tissues were too compliant and fragile to test in uniaxial tension. These tissues were frequently damaged during dissection and therefore the 1-week biomechanical results were not reported.

The material properties of the natural healing tissues also reached asymptotic values by 8 weeks post-surgery. Ultimate stresses transmitted by the 2-, 5-, and 8-week natural healing tissues increased from 40% to 68% to 69% of normal PT values, respectively ($p < 0.006$; Table II). The 2-week values were significantly less than the ultimate stresses for the 5- and 8-week time points. The moduli transmitted by the 2-, 5- and 8-week natural healing tissues also increased from 57% to 86% to 89% of normal PT, respectively, with the 8-week values being significantly greater than the 2-week moduli ($p < 0.006$). The modulus of the natural healing tissue at 2 weeks post injury was also the only healing time point that was significantly less than normal PT modulus ($p < 0.006$).

Structural properties for the contralateral sham groups were not different than normal (Table II, Fig. 5b). The material properties of the 2-week and 5-week shams were not different than normal. However, ultimate stress and modulus for the 8-week sham group was significantly higher than values for the normal PT ($p < 0.006$).

DISCUSSION

The objective of this study was to investigate changes in spatial Col1 and Col2 gene expression, tissue morphology and natural healing biomechanics over time following creation of a full-length, central PT injury. The natural healing tissue did not generate normal cellular or matrix organization by 5 weeks post-surgery or normal tissue biomechanics by 8 weeks post-surgery. A typical wound healing response was seen with hemostasis, inflammation, proliferation and remodeling stages.[15] We found an influx of inflammatory cells at 1 week consistent with previous work in a lamb central-third PT defect model.[16] Also consistent with our study, Sanchis-Alfonso et. al. found a disorganized matrix and hypercellular tissue at 2 weeks post-surgery with increased collagen matrix and reduced cellularity by 3 weeks. Although both studies showed further matrix remodeling and collagen fiber alignment along the primary axis of the tendon between 3 and 5 weeks, our results also revealed inferior repair biomechanics.

Most studies, including the current results, report linear stiffness and ultimate load to failure rather than repair properties in a lower-force, more functional region of loading. We have recorded peak *in vivo* forces of 21% and 40% of normal PT failure forces in the rabbit[11] and goat[17] models, respectively, for activities of daily living (ADLs) to create benchmarks for our tissue-engineered repairs. Since the extremely small size of the mouse knee prevents us

from directly and accurately measuring murine PT forces, we have chosen to apply these design limits across species based on expected ADLs (Fig. 5a). ***21% of Normal Failure Load (0.88N).*** The 2-week natural healing tissue was functionally inadequate as it did not mimic normal tangent stiffness but required an additional displacement of 0.18mm to achieve 0.88N ($p<0.05$). By 5 weeks, however, the healing tissue was not significantly different than normal ($p>0.05$). The 8-week defect healing tissue actually matched normal PT tangent stiffness within this range. ***40% of Normal Failure Load (1.65N).*** The natural healing tissues at all three time points were inadequate requiring at least an additional 0.123mm of displacement (4% strain) to reach 1.65N. In fact, only 33%, 75%, and 69% of the samples at 2-, 5-, and 8-weeks, respectively, exhibited failure forces equal to or higher than this 40% level. This additional analysis further demonstrates the functional inadequacies of adult natural tendon healing in this murine model.

Multiple studies have looked at natural healing of full-length, central PT tendon defects in rabbits,[9] dogs,[18] and lambs[16] with varying biomechanical outcomes. Differences in surgical procedure, mechanical testing and analysis methods can contribute to these differences but other species- or size-related factors may have an even greater impact. We have attempted to compare biomechanical healing between central patellar tendon injuries in the mouse and rabbit, with average life-spans of approximately 2 years and 6–7 years, respectively. To better compare healing between these two species, we normalized time post-surgery to age at the time of surgery. Although it is apparent when mapping percent of normal force vs. normalized healing time (Fig. 6) that the mouse heals better and faster than the rabbit, several confounding factors could affect these outcomes. For instance, while the relative defect size compared to the overall tendon volume is similar in both models, the absolute defect volume in the rabbit model is 180X greater than in the mouse. As type-I collagen structure is likely homologous between species, the rabbit must produce and assemble far more ECM, potentially contributing to its slower and less complete healing response. The increased metabolism of the mouse combined with its lower tissue forces could also benefit defect healing. These comparisons are important as researchers attempt to translate tendon healing and tissue engineered findings to larger preclinical models.

There were limitations in this study. 1) Using a scalpel blade to create the insertional injury did not ensure that the entire insertion was removed. This limitation could have produced inconsistent spatial healing depending on where the scalpel injured the bone. This could also account for the minimal Col2 expression seen at these insertion injuries. We plan to use a surgical burr in future studies to uniformly disrupt the insertion within the central defect. This method of creating a consistent injury between species is necessary as we try to better mimic the bony trough created in our central-third NZW rabbit PT defect model.[9, 12, 19] 2) Due to the limited size of the tendon, we could not mark the boundaries of the defect during surgery as we did when creating the rabbit PT defect injury.[9, 12, 19] Instead, we relied on the discoloration of the defect region when removing the medial and lateral struts during dissection prior to mechanical testing. Any remaining strut on the test specimen could have led to overestimates of actual mechanical properties. 3) Slipping occurred within the patellar grip during the uniaxial failure tests in a limited number of samples. The slippage typically occurred between 1.5N and 2.5N of load. Therefore, displacement and strain at failure were not reported and stiffnesses were calculated from the linear region prior to slipping. 4) Optical strain measurements were not taken during the biomechanical tests, as tissue markers were difficult to apply to the fragile healing tissue. Therefore, average modulus was reported over the full tissue length. Future studies will utilize ink markers to measure local strains.

Given its genetic power, the murine full-length PT defect injury serves as a potent tool for biological and biomechanical study of natural tendon healing. While its limited size may

prevent examination of certain novel tissue engineering treatments, advances made in the murine model could conceivably be translated into larger models where repeatable surgeries and design benchmarks are possible. Developing such analogs is particularly attractive if similar biomechanical and/or biological responses to injury can be identified.

Just as functional tissue engineers have been developing mechanical success criteria, corresponding biological success criteria will be needed as well. Murine injury models allow measurement of such biological success criteria by comparing the expression of tenogenic markers in natural healing tissue to normal adult tendon as well as normal tendon during embryonic and early post-natal development. These comparisons are expected to provide multi-functional design benchmarks for tissue-engineered therapies. Such strategies have the potential to promote tenogenesis and zonal insertion regeneration rather than non-functional scar formation and inferior repair biomechanics.

Supplementary Material

Refer to Web version on PubMed Central for supplementary material.

Acknowledgments

This study was funded by National Institutes of Health grants AR46574-07 and AR56943-01. We also thank Drs. Lou Soslowsky and David Glaser for their help in designing the mechanical testing grips used in this study and Drs. Al Banes and Greg Boivin for histological assistance.

REFERENCES

1. Praemer, A.; Furner, S.; Rice, D. Musculoskeletal conditions in the United States. Second ed.. Parke Ridge, IL: American Academy of Orthopaedic Surgeons; 1999.
2. Rees JD, Wilson AM, Wolman RL. Current concepts in the management of tendon disorders. Rheumatology. 2006; 45:508–521. [PubMed: 16490749]
3. Thomopoulos S, Marquez J, Weinberger B, et al. Collagen fiber orientation at the tendon to bone insertion and its influence on stress concentrations. J Biomech. 2006; 39:1842–1851. [PubMed: 16024026]
4. Galatz L, Rothermich S, VanderPloeg K, et al. Development of the supraspinatus tendon-to-bone insertion: Localized expression of extracellular matrix and growth factor genes. J Orthop Res. 2007; 25:1621–1628. [PubMed: 17600822]
5. Benjamin M, Toumi H, Ralphs J, et al. Where tendons and ligaments meet bone: Attachment sites ('entheses') in relation to exercise and/or mechanical load. J Anat. 2006; 208:471–490. [PubMed: 16637873]
6. Fung D, Wang V, Andarawis-Puri N, et al. Early response to tendon fatigue damage accumulation in a novel in vivo model. J Biomech. 2010; 43:274–279. [PubMed: 19939387]
7. Bedi A, Kovacevic D, Hettrich C, et al. The effect of MMP inhibition on tendon-to-bone healing in a rotator cuff repair model. J Shoulder Elbow Surg. 2010; 19:384–391. [PubMed: 19800260]
8. Jelinsky S, Lake S, Archambault J, Soslowsky L. Gene expression in rat supraspinatus tendon recovers from overuse with rest. Clin Orthop Relat Res. 2008; 466:1612–1617. [PubMed: 18459028]
9. Awad HA, Boivin GP, Dressler MR, et al. Repair of patellar tendon injuries using a cell-collagen composite. J Orthop Res. 2003; 21:420–431. [PubMed: 12706014]
10. Carpenter JE, Hankenson KD. Animal models of tendon and ligament injuries for tissue engineering applications. Biomaterials. 2004; 25:1715–1722. [PubMed: 14697872]
11. Juncosa N, West J, Galloway M, et al. *In vivo* forces used to develop design parameters for tissue engineered implants for rabbit PT repair. J Biomech. 2003; 36:483–488. [PubMed: 12600338]

12. Juncosa-Melvin N, Shearn J, Boivin G, et al. Effects of mechanical stimulation on the biomechanics and histology of stem cell-collagen sponge constructs for rabbit patellar tendon repair. Tissue Eng. 2006; 12:2291–2300. [PubMed: 16968169]

13. Chokalingam K, Juncosa-Melvin N, Hunter S, et al. Tensile stimulation of murine stem cell-collagen sponge constructs increases collagen type I gene expression and linear stiffness. Tissue Eng Part A. 2009; 15:2561–2570. [PubMed: 19191514]

14. Montgomery, C. Design and analysis of experiments. 7th ed.. John Wiley & Sons; 2008.

15. James R, Kesturu G, Balian G, Chhabra A. Tendon: Biology, biomechanics, repair, growth factors, and evolving treatment options. J Hand Surg Am. 2008; 33:102–112. [PubMed: 18261674]

16. Sanchis-Alfonso V, Subias-Lopez A, Monteagudo-Castro, et al. Healing of the patellar tendon donor defect created after central-third patellar tendon autograft harvest. Knee Surg Sports Traumatol Arthrosc. 1999; 7:340–348. [PubMed: 10639650]

17. Korvick DL, Cummings JF, Grood ES, et al. The use of an implantable force transducer to measure patellar tendon forces in goats. J Biomech. 1996; 29:557–561. [PubMed: 8964786]

18. LaPrade R, Hamilton C, Montgomery R, Wentorf F, Hawkins H. The reharvested central third of the patellar tendon. Am J Sports Med. 1997; 25:779–785. [PubMed: 9397265]

19. Butler DL, Juncosa-Melvin N, Boivin GP, et al. Functional tissue engineering for tendon repair: A multidisciplinary strategy using mesenchymal stem cells, bioscaffolds, and mechanical stimulation. J Orthop Res. 2008; 26:1–9. [PubMed: 17676628]

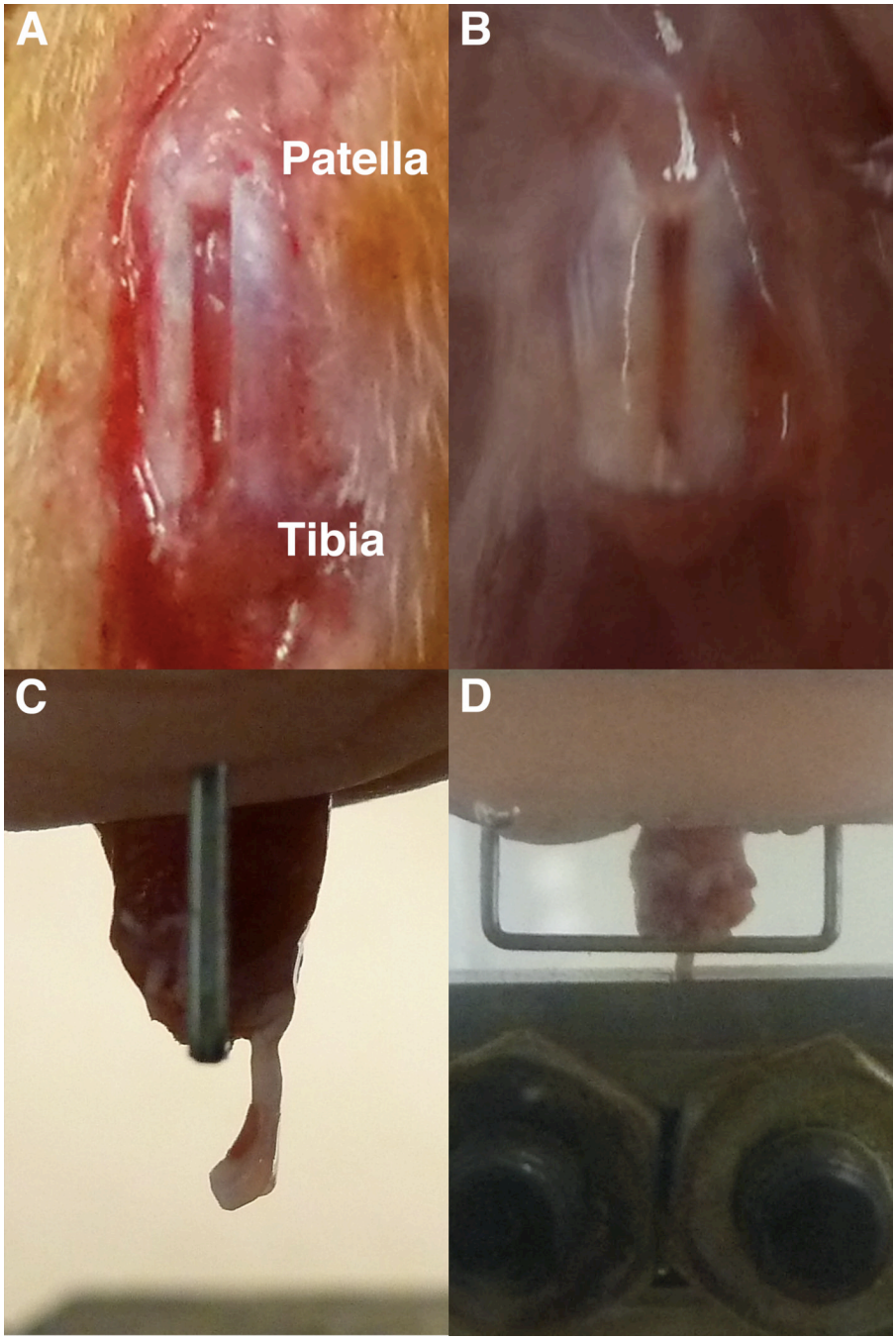

Fig. 1.
The full-length, central PT defect just following surgery (a) becomes discolored during healing (b). During mechanical testing, the sample was mounted in the tibial grip (c) aided with bone cement and a staple. It was then lowered into the patella grip (d) in the testing system.

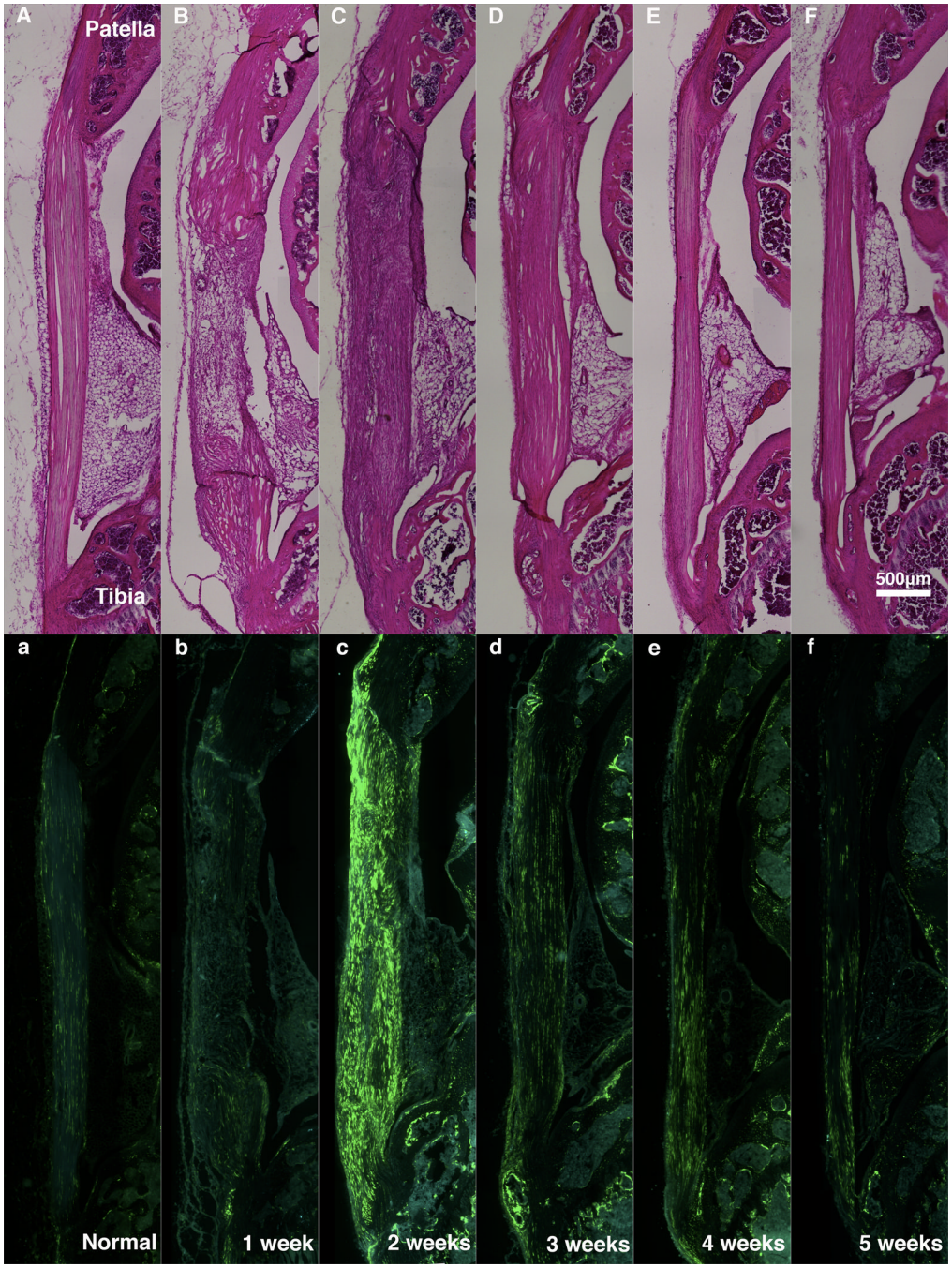

Fig. 2.

H&E (A–F) and Col1-GFPtpz/Col2-ECFP (a–f) micrographs from serial sagittal sections from Normal PT (A,a) and the defect region at one (B,b), two (C,c), three (D,d), four (E,e) and five (F,f) weeks of healing.

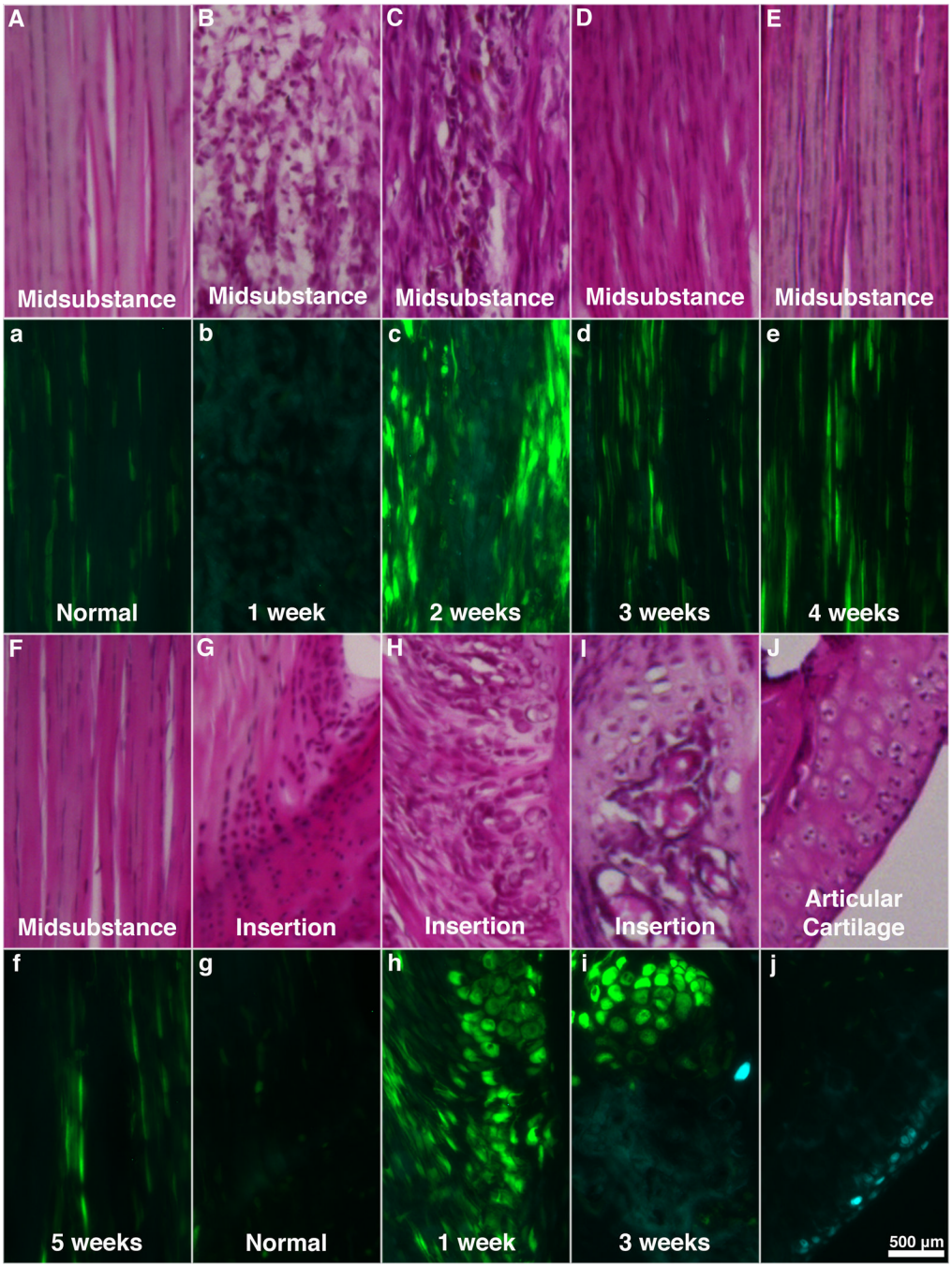

Fig. 3.

Serial H&E and Col1-GFPtpz/Col2-ECFP micrographs from the midsubstance (A–F, a–f) and tibial insertion (G–I, g–i) from normal PT (A,a,G,g) and the defect region at one (B,b,H,h), two (C,c) three (D,d,I,i), four (E,e) and five (F,f) weeks of healing. (J,j) Col2 expression can be seen within chondrocytes in articular cartilage beneath the patella.

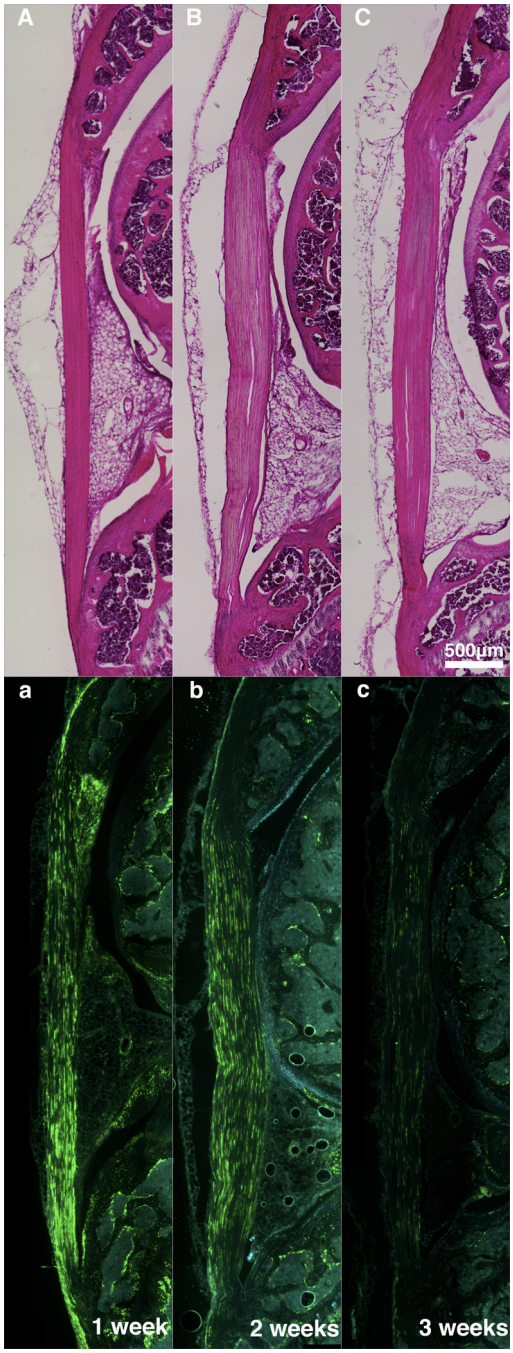

Fig. 4.

Serial H&E and Col1-GFPtpz/Col2-ECFP micrographs of contralateral sham limbs at one (A,a), two (B,b), and three (C,c) weeks depicting an increase in Col1 expression at 1-week that reduces to normal PT levels by 3-weeks post-surgery. Four and five weeks data not shown but were consistent with the 3 week time point.

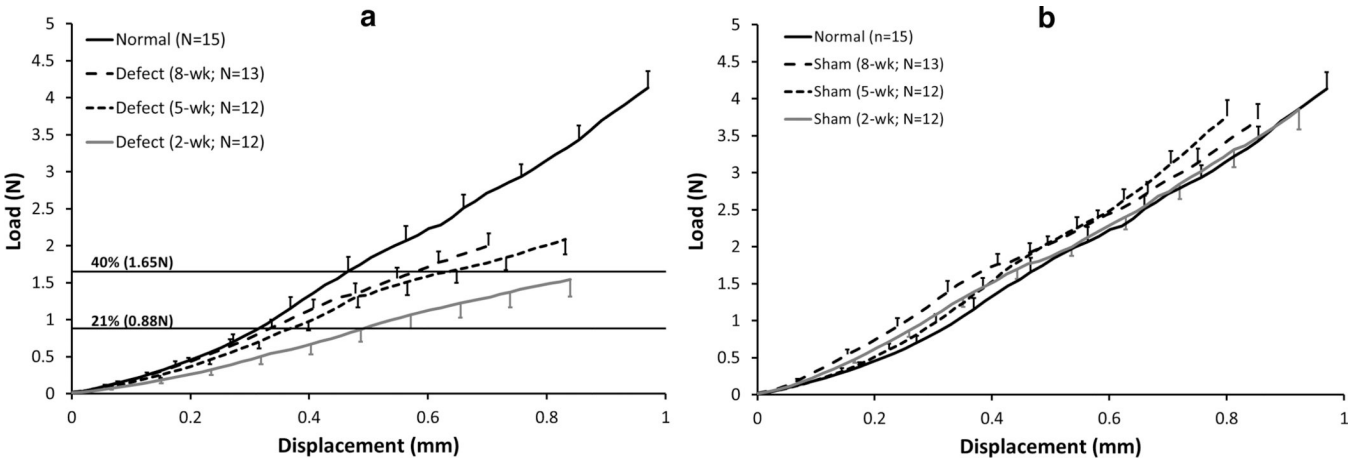

Fig. 5.

Average load-displacement curves. (a) The healing tissue showed significantly decreased structural properties at 2-, 5-, and 8-weeks compared to normal PT ($p < 0.05$). There were no significant differences among the healing tissues at any time point. The corresponding displacements at force levels recorded in the rabbit PT (21% of normal)[11] and the goat PT (40% of normal)[17] showed that the healing tissues were too compliant and not functional to 40% levels even after 8 weeks of healing. (b) The contralateral shams had no effect on structural properties at any time point when compared to normal PT, except the stiffness for the 2-week sham which was greater than normal ($p = 0.02$). Error bars indicate SEM.

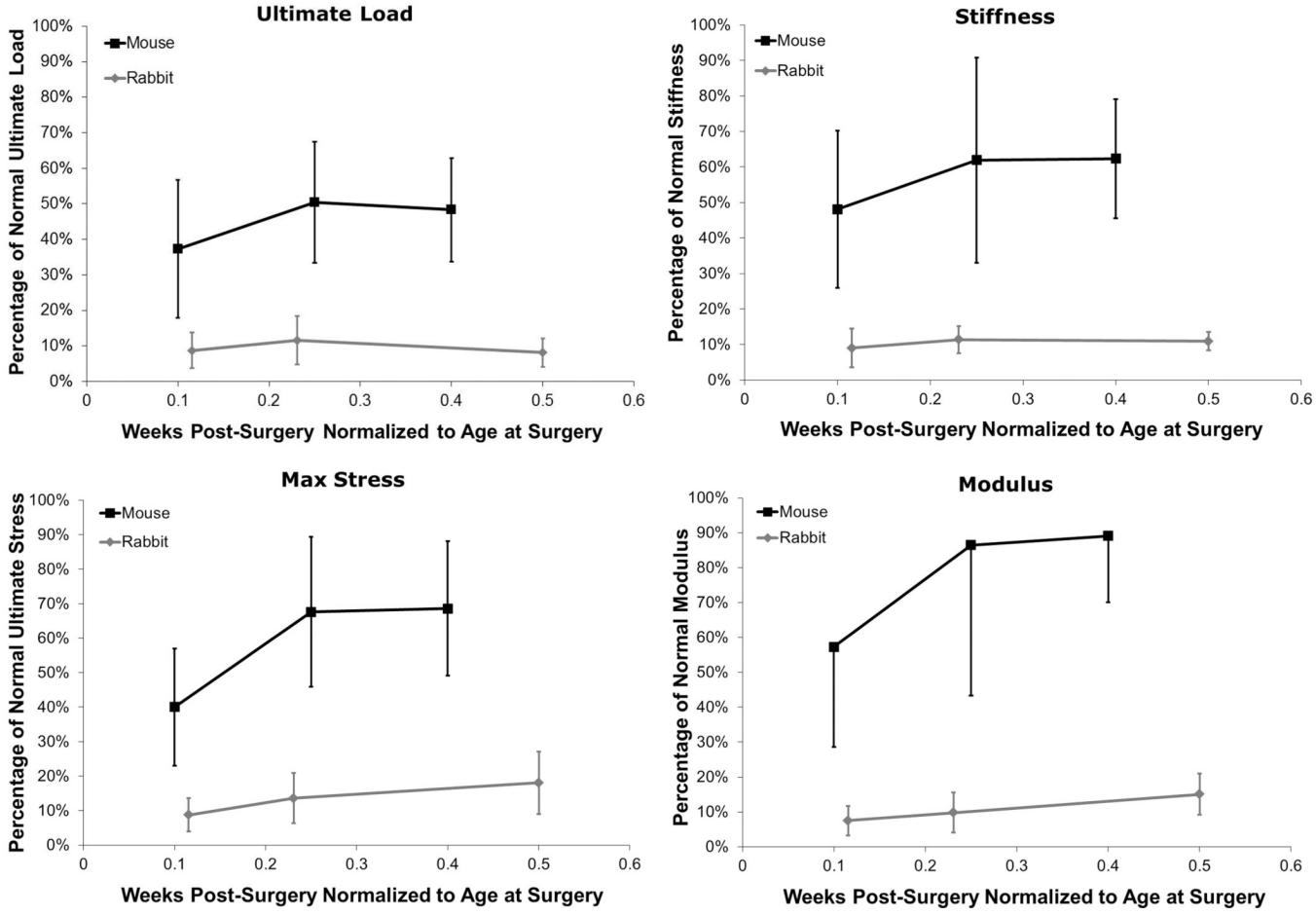

Fig. 6.

Comparisons of ultimate load, stiffness, ultimate stress, and modulus vs. time post-surgery normalized to the age at surgery showed improved healing in the mouse model vs previous work done in the rabbit central-third defect model.[9] Error bars indicate SD.

Table I

Experimental Design – Healing tissue within full-length central PT defects were compared to contralateral shams and age-matched normals for histology and biomechanics

		Time Post-Surgery (weeks)						
Treatment		**0**	**1**	**2**	**3**	**4**	**5**	**8**
Defect	Histology		3	3	3	3	3	
	Biomechanics		12	12			12	13
Sham	Histology		3	3	3	3	3	
	Biomechanics		12	12			12	13
Normal PT	Histology	3						
	Biomechanics	15						

Table II

Structural and material properties of the defect tissue compared to contralateral shams and age-matched normal PT (mean±SD)

	Ultimate Load (N)	Stiffness (N/mm)	Ultimate Stress (MPa)	Modulus (MPa)
Defect (2-wk, N=12)	1.54±0.81*	3.26±1.50*	4.67±1.99*	32.37±16.17*
Sham (2-wk, N=12)	3.85±0.92	5.26±0.77	14.17±4.06	60.12±20.48
Defect (5-wk, N=12)	2.08±0.70*	4.20±1.96*	7.90±2.53*§	48.85±24.39
Sham (5-wk, N=12)	3.76±0.76	7.22±0.91	13.80±4.93	79.47±23.51
Defect (8-wk, N=13)	2.00±0.60*	4.23±1.14*	8.01±2.28*§	50.35±10.79§
Sham (8-wk, N=13)	3.73±0.73	6.38±1.48	17.64±2.91*	90.57±19.18*
Normal PT (N=15)	4.13±0.87	6.78±2.05	11.68±3.38	56.51±18.29

*significantly different from age-matched Normal PT,

§significantly different than Defect (2-wk) – bonferroni-corrected ($p < 0.006$) significant differences are noted above only for comparisons against normal and comparisons among the defect groups over time